Molecular Phylogenetics and Evolution 201 (2024) 108192

Contents lists available at ScienceDirect

Molecular Phylogenetics and Evolution

journal homepage: www.elsevier.com/locate/ympev

Evolution of chitin-synthase in molluscs and their response to ocean acidification

Maoxiao Peng [a], João C.R. Cardoso [a,*], Deborah M. Power [a,b,c,*]

[a] Comparative Endocrinology and Integrative Biology, Centre of Marine Sciences, Universidade do Algarve, Campus de Gambelas, 8005-139 Faro, Portugal
[b] International Research Center for Marine Biosciences, Ministry of Science and Technology, Shanghai Ocean University, Shanghai, China
[c] Key Laboratory of Exploration and Utilization of Aquatic Genetic Resources, Ministry of Education, Shanghai Ocean University, Shanghai, China

ARTICLE INFO

Keywords:
Biomineralization
Chitin-synthase evolution
Mollusc
Ocean acidification
Species-specific functional diversification

ABSTRACT

Chitin-synthase (CHS) is found in most eukaryotes and has a complex evolutionary history. Research into CHS has mainly been in the context of biomineralization of mollusc shells an area of high interest due to the consequences of ocean acidification. Exploration of *CHS* at the genomic level in molluscs, the evolution of isoforms, their tissue distribution, and response to environmental challenges are largely unknown. Exploiting the extensive molecular resources for mollusc species it is revealed that bivalves possess the largest number of *CHS* genes (12–22) reported to date in eukaryotes. The evolutionary tree constructed at the class level of molluscs indicates four *CHS* Type II isoforms (A-D) probably existed in the most recent common ancestor, and Type II-A (Type II-A-1/Type II-A-2) and Type II-C (Type II-C-1/Type II-C-2) underwent further differentiation. Non-specific loss of *CHS* isoforms occurred at the class level, and in some Type II (B-D groups) isoforms the myosin head domain, which is associated with shell formation, was not preserved and highly species-specific tissue expression of *CHS* isoforms occurred. These observations strongly support the idea of CHS functional diversification with shell biomineralization being one of several important functions. Analysis of transcriptome data uncovered the species-specific potential of *CHS* isoforms in shell formation and a species-specific response to ocean acidification (OA). The impact of OA was not *CHS* isoform-dependent although in *Mytilus*, Type I-B and Type II-D gene expression was down-regulated in both *M. galloprovincialis* and *M. coruscus*. In summary, during *CHS* evolution the gene family expanded in bivalves generating a large diversity of isoforms with different structures and with a ubiquitous tissue distribution suggesting that chitin is involved in many biological functions. These findings provide insight into *CHS* evolution in molluscs and lay the foundation for research into their function and response to environmental changes.

1. Introduction

Chitin is a widespread amino polysaccharide found in nature. It is a homopolymer of β-1,4-N-acetyl-D-glycosamine and part of the structure of a diversity of animal and plant tissue and provides resistance and strength. It is an important scaffolding material of fungi and yeast cell walls and a major component of arthropod exoskeletons (20–30 % of the crustacean carapace) (Kramer and Koga, 1986; Muzzarelli, 2013). In vertebrates, chitin is absent from mammals and birds, but it exists in fish scales and has also been detected in fish and amphibian larvae suggesting that this polymer has multiple roles in vertebrate biology (Tang et al., 2015). The process by which animals synthesize chitin has raised a lot of interest not only because of its diverse applications (Desbrières and Guibal, 2018) but also because of its role as a major component of the protective exoskeleton of marine invertebrates. For example, although chitin is a relatively minor constituent of mollusc shells its role as a scaffold means a change in its production caused by environmental conditions such as ocean acidification is likely to significantly effect this phylum.

The molluscs are the second-largest phylum of invertebrate animals after the arthropods and inhabit terrestrial and aquatic environments. Most molluscs possess a mineralized shell that regulates ion homeostasis and confers protection. The composition of the shell is fairly well characterised, and it is mostly composed of calcium carbonate crystals in an organic matrix composed of proteins and to a lesser extent the complex polysaccharide, chitin (Falini et al., 1996; Marin et al., 2012;

* Corresponding authors.
E-mail address: dpower@ualg.pt (D.M. Power).

https://doi.org/10.1016/j.ympev.2024.108192
Received 19 June 2024; Received in revised form 28 August 2024; Accepted 5 September 2024
Available online 8 September 2024

Suzuki and Nagasawa, 2013). However, shell production by the mantle and haemocytes remains poorly understood. The last common ancestor of the Conchifera (shell bearing molluscs) possess chitin, the concentration of which varies with the stage of differentiation of the shell (Furuhashi et al., 2009). Chitin is proposed to constitute 3.5 % of the shell matrix (Chan et al., 2018; Heredia et al., 2007) and forms the scaffold for crystal mineralization (Falini et al., 1996). The calcium carbonate crystals in the shell are aligned with the chitin fibres (Weiner et al., 1983; Weiner and Traub, 1980) but how chitin is produced and regulated to form the cross-linked matrix essential for shell growth and maintenance remains unresolved. Insights into the evolution and regulation of the complex of proteins that produce, and breakdown chitin may provide insight into its role in mollusc shell formation.

Chitinases and chitin synthase (CHS) are two groups of enzymes that determine the breakdown and formation of the chitin fibres, respectively. *CHS* is only found in species containing chitin but chitinases are widespread and exist in viruses through to mammals (Gooday, 1999). CHS belongs to family 2 of the glycosyltransferase (Merzendorfer, 2011) and synthesize the chitin polymer and are involved in the addition of UDP-GlcNac units to the growing oligosaccharide chain (Falini and Fermani, 2004). In vertebrates *CHS* has only been reported in fish and amphibians but they are common in invertebrate metazoan. In fungi *CHS* are very diverse and family members are grouped into seven distinct classes (Roncero, 2002) but in metazoan they are less numerous, and their evolutionary relationship is complex. The independent fusion of different myosin motor domains (myosin head) with CHS is common in lophotrochozoans and fungi and at least 5 gene duplication events are proposed to have occurred during *CHS* evolution in metazoan (Zakrzewski et al., 2014).

CHS have been isolated from the rigid pen shell (*Atrina rigida*) (Weiss et al., 2006), the Japanese pearl oyster (*Pinctada fucata*) (Suzuki et al., 2007) and the Pacific oyster (*Magallana gigas*) (Zhang et al., 2019). The owl limpet *Lottia gigantea* is proposed to have the highest *CHS* gene number (10 isoforms), but recent research indicates that amphioxus has 11–12 *CHS* isoforms (Shi et al., 2020). Analysis of publicly available genome data for molluscs, reveals numerous *CHS* isoforms in bivalves. The extensive *CHS* diversification, and variety of chitinous structures in Mollusca mineralization, suggests that specific interactions of CHS with minerals may influence shell formation.

Relatively few studies have considered the functional dependence of CHS on the extracellular microenvironment (Weiss, 2012; Weiss et al., 2013; Zhang et al., 2019). Furthermore, the likely effect of environmental conditions on the evolution of *CHS* isoforms, tissue distribution, and function in the speciose molluscs is unclear. In this study CHS in molluscs was characterized and this enzyme's putative role in mollusc shell construction was determined. Taking advantage of assembled transcriptome data for the Mediterranean mussel (*Mytilus galloprovincialis*) and publicly available data for the evolutionary proximate hard-shelled mussel (*Mytilus coruscus*) and the more distant Pacific oyster (*M. gigas*), CHS expressed in the mantle was characterized under control and OA conditions.

2. Material and methods

2.1. Database searches and protein domain prediction

CHS sequences from oyster (*M. gigas*) were used to retrieve from public databases putative *CHS*-like genes/transcripts (*e-value* $\leq$ 1e $^{-40}$) from 39 representative species of the Fungi kingdom and animal phyla Porifera, Cnidaria, Mollusca, Arthropoda, and Chordata (**Supplementary Table 1**). Additional sequence resources were identified in deduced protein sequences of genes by domain analysis (Pfam database, https://pfam.xfam.org) focused on 1) the Chitin_synth_2 domain, and 2) a transmembrane domain and they were displayed using Tbtools software (Chen et al., 2020).

2.2. Sequence alignments and phylogenetic analysis

The MUSCLE algorithm (Edgar, 2004) in Aliview software (v 1.28) was used to generate multiple sequence alignments (MSA). The MSA was manually edited to remove gaps and improve alignments and used to construct Maximum Likelihood (ML) and Bayesian Inference (BI) phylogenetic trees. The ML tree was built in PhyML 3.0 using the ATGC bioinformatics platform (http://www.atgc-montpellier.fr/phyml/) with SMS automatic model selection (the most suitable model tested and used was the VT substitution model) and a 1,000 bootstrap replicates was used to study protein evolution (with Akaike Information Criterion, AIC). MrBayes v3.2 was used to build the BI tree using a VT substitution model (Aamodel = VT, obtained from SMS automatic model selection of ML tree; Samplefreq = 500; relburnin = yes, burninfrac = 0.25) with 1,000,000 generations. FigTree 1.4.3 (http://tree.bio.ed.ac.uk/software/figtree) was used to display trees and was rooted with Fungi *CHS* and edited in the Inkscape program (https://inkscape.org). Functional motifs of the Chitin_synth_2 domain, the donor saccharide binding site (DSBS), acceptor saccharide binding site (ASBS) and product binding site (PBS) were analysed to identify functional motifs and displayed using Tbtools software (Chen et al., 2020). According to Morozov and Likhoshway's (2016) and Zakrzewski et al., (2014) the evolution of CHS in eukaryotes can be divided into two main branches: CHS type I and CHS type II. We categorized the CHS and named the subbranches within the two branches according to the order in which the branches appeared in the evolutionary tree.

2.3. Species orthogroup inference and gene mapping

Protein datasets from the genomes of seventeen bivalve species (**Supplementary Table 2**) were used for species phylogenetic tree analysis. Alternative transcripts were removed from the initial protein data set obtained for each species. The protein database and gff annotation file of the species genomes were used to extract primary transcripts in the sequence toolkit of the TBtools software (Chen et al., 2020). Global orthogroup resolution was performed using Orthofinder (ver 2.5.4, parameters −M STAG; −T raxml) (Emms and Kelly, 2019). The species phylogenetic tree was displayed in FigTree 1.4.3 (http://tree.bio.ed.ac.uk/software/figtree).

The chromosome-level genomes of *M. gigas* (GCA_902806645.1), *M. coruscus* (GCA_017311375.1) and *M. galloprovincialis* (GCA_025277285.1) were used to construct the chromosomal location of *CHS* genes. The *CHS* chromosomal location information of *M. gigas* was obtained from the annotation of the genome, but positional information for *M. coruscus* and *M. galloprovincialis* was obtained by blast (blastn, cutoff setup: e-value < 1e^{-40}, identity > 99 %, coverage > 99 %) of the coding sequence (CDS) against the genome. The figures of *CHS* mapped to the genome were prepared using chromoMap and the gggenes package in R-studio.

2.4. Acidification assay and mantle transcriptome sequencing of *M. galloprovincialis* and *M. gigas*

The *M. coruscus* mantle transcriptome data from animals exposed to OA was downloaded from NCBI and published by Zhao et al., (2020) (for the accession number see **Supplementary Table 2**). The mantle samples and transcriptome data of *M. galloprovincialis* and *M. gigas* after OA treatment were from a previous experimental study by the authors (Peng et al., unpublished). In brief, juvenile Mediterranean mussels (*M. galloprovincialis,* 3.0–3.5 cm shell-length and 8.62–10.11 g weight) were collected from the Ria Formosa (Faro, Portugal, ICNF license 327/2022/CAPT). The juvenile Pacific oysters (*M. gigas*, 3.0–3.5 cm shell-length and 5.23–6.11 g weight) were obtained from a local company Bivalvia (Olhão, Portugal). Experiments were performed in an open circuit system under normal environmental conditions of photoperiod and temperature (13–17 °C) for November-January in the Algarve

(Portugal). Seawater was acidified in header tanks by pumping in CO_2 gas under controlled conditions to decrease the ambient pH value from, pH 8.2 to pH 7.8. The response of the bivalves was established after 60 days exposure to OA at the pH predicted for the year 2100 (pH 7.8; (Hönisch et al., 2012)). The seawater temperature, oxygen, and pH of the circuits were continuously monitored, and fluctuations automatically corrected (Aquatronica, Reggio Emilia, Italy). Triplicate aquaria (each aquaria contained n = 10 mussels and n = 9 oysters) were established for ambient seawater pH 8.2 (control, SW) and seawater at pH 7.8 (OA) conditions. Mussels and oysters were exposed to the OA challenge for 60 days in an open circuit supplied with aerated seawater (pH 8.19 ± 0.01) and with seawater gassed with CO_2 to achieve the desired pH, 7.8 ± 0.01. Animals were fed daily with dried microalgae (PHYTOBLOOM, Necton, Portugal), which was added to each experimental tank to give a final approximate concentration of 0.2 mg of microalgae/individual bivalve. After mussels and oysters were exposed to the experimental conditions for 60 days, samples of the posterior mantle edge of the left valve were collected frozen on dry ice and stored at −80 °C for total RNA extraction (tRNA). No mortality of bivalves occurred during the experiment.

tRNAs from mussels and oysters were used for transcriptome sequencing, and only tRNA from mussels was used for quantitative expression analysis (qPCR) expression assays because the *CHS* gene did not respond significantly in oysters. The experimental method and steps for tRNA extraction from samples were the same as reported in previous studies (Peng et al., 2023).

After OA exposure mantle transcriptome sequencing of *M. galloprovincialis* and *M. gigas* were as reported in a previous study by us (Peng et al., unpublished). In brief, samples used for transcriptome library construction consisted of a pool of tRNA (2 μg) from two (2) individuals/ experimental group (1 μg of tRNA/animal) and three (3) replicate samples per treatment group. Library preparation and sequencing were outsourced to the Experimental Department of Novogene (Beijing, China). Sequencing was carried out using an Illumina TrueSeq mRNA-Seq library Prep kit and sequenced on an Illumina Novaseq 6000 and 150 bp paired-end raw-reads were generated. The transcriptome raw data have been uploaded to the NCBI database, and the data accession number is shown in **Supplementary Table 2.**

2.5. Expression analysis

The transition of the trochophore larva to a D shaped larva is the stage at which the bivalve shell emerges. The *CHS* genes expression of *M. gigas*, *M. galloprovincialis* and *M. coruscus* in tissues, larva and mantle (with OA exposure) are based on transcriptome data analysis. The raw transcriptome data are from the NCBI public database (OA mantle transcriptome data described above), and details about the raw data are provided in **Supplementary Table 2**. Transcriptome data were analyzed to obtain the transcript FPKM values using the procedure reported in (Peng et al., 2023).

qPCR was used to examine *M. galloprovincialis CHS* genes that significantly responded to OA. Mantle cDNA was prepared from 6 individuals of each experimental group. DNase treated mantle tRNA (500 ng) was used for cDNA synthesis for qPCR. The reaction mix consisted of 10 ng of random hexamers (pd(N)6, Jena Bioscience, Germany), dNTPs (2 mM, ThermoScientific, USA), 100 U of RevertAid Reverse Transcriptase, 8 U Ribolock RNAse inhibitor (ThermoScientific) in a reaction volume of 20 μl.

SsoFast EvaGreen Supermix (Bio-Rad, Portugal) was used for the qPCR reactions, which contained 200 nM of candidate gene specific primer pairs (**Supplementary Table 3**) and 2 μl of cDNA template in a final reaction volume of 10 μl. Duplicate reactions were used for all samples (n = 6 for each experimental group) and controls (accepting < 5 % variation between replicates) and all reactions were run on a Real-Time PCR Detection System for 96-well microplates (CFX Connect, Bio-Rad). Non-specific PCR products and primer dimers were detected by running melting curves (60 – 95 °C) at the end of each PCR. To confirm the absence of contaminating genomic DNA or contamination due to technical failures, reverse transcriptase (RT-) and PCR control (no template) reactions, respectively were included in qPCR assays. The efficiency of the designed PCR primer pairs was determined, and serial dilutions of purified amplicons were used to establish the coefficient of determination (R^2) for PCR assays. Elongation factor 1-alpha (EF1α) and 18S ribosomal RNA, which had a constant expression in *M. galloprovincialis* irrespective of the treatments, were used as the reference genes for normalization. Quantification was based on the standard curve method.

2.6. Statistical analysis

Statistical analysis was implemented in SPSS 19.0 with the p-value cut-off for significance set at 0.05. For the qPCR assays the results are presented as the mean of 6 replicates ± SEM for each condition. Significant differences in gene expression (qPCR data and FPKM values from transcriptome data) between the samples of the OA and control group were identified by applying a two-tailed Student's *t*-test.

3. Results

3.1. Phylogenetic tree and distribution of chitin-synthase isoform

A species phylogenetic tree was constructed using protein sequences obtained from the whole genome of seventeen species in 8 classes of the phylum Mollusca (Fig. 1). Detected *CHS* gene copies revealed that the *CHS* gene family expanded in the Mollusca. Due to the limited availability in public databases of DNA sequences from the Solenogastres, Caudofoveata, Polyplacophora, Scaphopoda, and Monoplacophora classes, only a single representative species from each class was analyzed and yielded 4–7 *CHS* isoforms (Table 1). The genomes of two species of the Cephalopoda class yielded 11–12 *CHS* isoforms, examination of the genome of four species of the Gastropoda class, yielded 8–12 *CHS*, and analysis of the genome of six species of the Bivalvia class, yielded 12–22 *CHS* isoforms.

A phylogenetic tree was constructed from a total of 228 deduced CHS amino acid sequences from the genomes of 39 species (Fig. 2 **and Supplementary Fig. 1**). The CHS sequences were from Fungi, Porifera, Cnidaria, Arthropoda, Chordata (Leptocardii, Actinopterygii, Ascidiacea and Amphibia), and Mollusca (Bivalvia, Gastropoda, Cephalopoda, Polyplacophora, Monoplacophora, Scaphopoda, Solenogastres and Caudofoveata).

The *CHS* genes duplicated in the metazoans and two major clades, Type I and Type II were identified and were expanded in molluscs. Type I and Type II *CHS* in molluscs underwent a further round of duplication generating Type I-A, I-B, II-A (II-A-1 and II-A-2), Type II-B, Type II-C (II-C-1 and II-C-2) and Type II-D clades. The *CHS* isoforms of the Porifera and Cnidaria phyla are exclusively distributed within the Type I-A branch. All Arthropod *CHS* were Type II-D isoforms and the Solenogastres and Polyplacophora classes lost gene isoforms of I-A, II-A, and II-D.

3.2. Sequence analysis of chitin-synthase isoform

All the sequences used for the phylogenetic tree and sequence analysis shared a conserved core CS2 (Chitin_synth_2) domain (**Supplementary Fig. 2**). The CHS of Fungi have different characteristics from the CHS of the metazoan species analysed in this study, specifically, they possess the CS1 domain (Chitin_synth_1N and Chitin_synth_1). Predicted transmembrane domains of Fungi CHS were restricted to the C-terminal side of the CS2 domain. However, the deduced protein of CHS of the metazoan species used in this study shared the transmembrane structural domain characteristic of Fungi CHS and possessed an additional transmembrane domain located in the

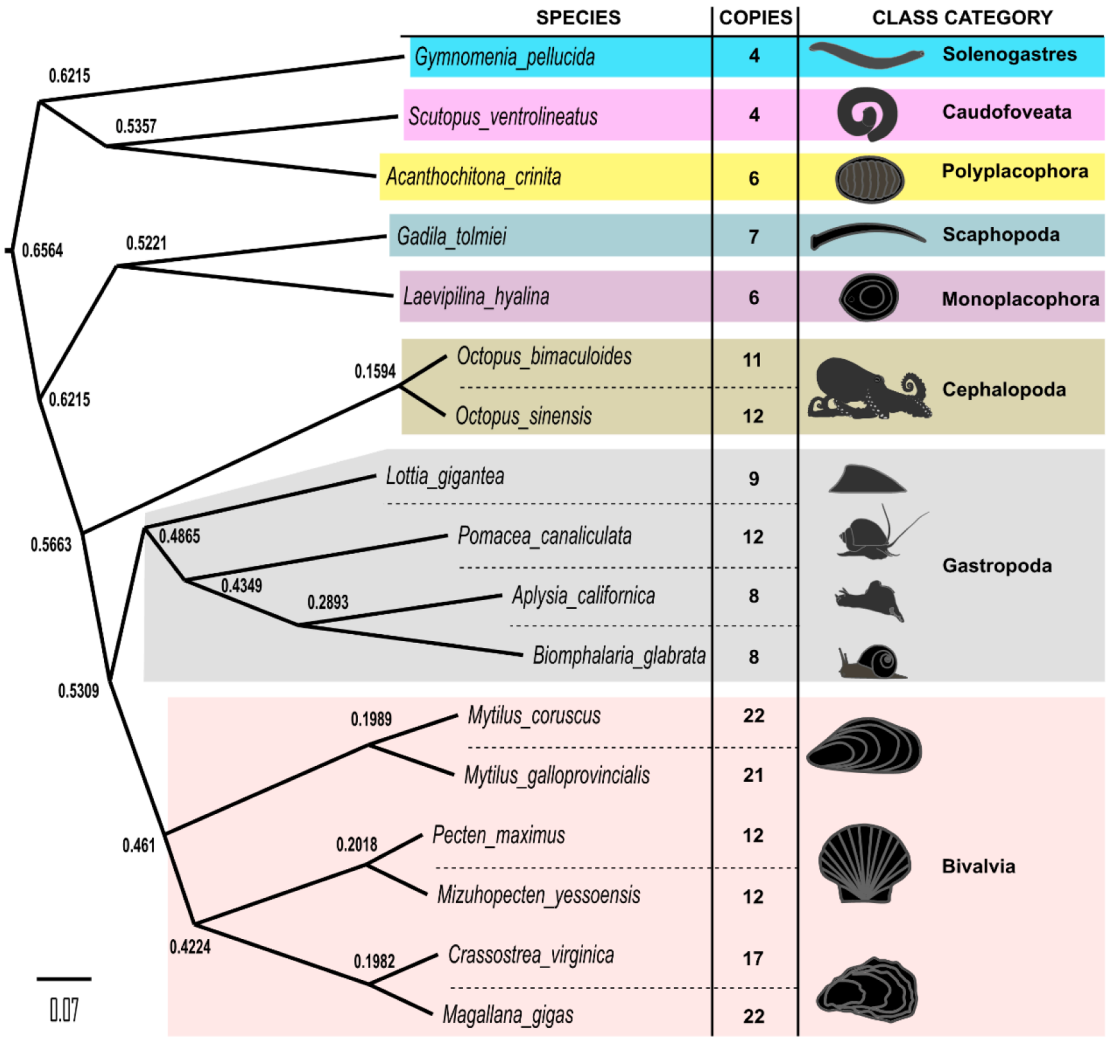

Fig. 1. Phylogenetic relationship of the mollusc species studied and the number of gene copies encoding chitin-synthase. Species evolutionary relationship inference was performed using the STAG method in Orthofinder (ver 2.5.4), which uses the proportion of species trees derived from single-locus gene trees that support each dichotomy as a measure of its support (node value). The species in which the genome was used to build the tree are indicated as well as the number of deduced *CHS* genes obtained from each species. Bivalves have the largest number of *CHS* gene isoforms.

N-terminal region (Fig. 3). The sterile alpha motif (SAM_1 and SAM_2) located in the C-terminal region was only identified in the Type I-A sequences, and the SAM_1 and SAM_2 domains generally appeared together. Exceptions were the Porifera, AquChsI1 (XP_003389565.3) and AquChsI2 (XP_003385441.1), where the SAM_1 and SAM_2 domains were absent. The N-terminal region of deduced CHS protein isoforms lacked a Myosin_head domain in Type I and Type II-A CHS and all CHS isoforms in the Arthropod and Chordata phylum (Fig. 3A). Almost all Type II-B, Type II-C, and Type II-D CHS isoforms contained the Myosin_head domain (**Supplementary Fig. 2**).

A donor saccharide binding site (DSBS), an acceptor saccharide binding site (ASBS) and a product binding site (PBS) were identified in the CS domain (Fig. 3B). Highly conserved ASBS (GEDRW) and PBS (QRRRW) motifs were found in all CHS isoforms of metazoan species included in this study. However, the conserved DSBS motif differed between Type I-A (DAD, GCFSVYR), Type I-B (DAD, GCFSLYR), and Type II (DGD, GCFSLFR) CHS isoforms (Fig. 3B **and** **Supplementary Fig. 3**).

The *CHS* genes identified in the genomes of the mussels (*M. galloprovincialis* and *M. coruscus*) and oyster (*M. gigas*) were present on different chromosomes, which contained multiple *CHS* genes (Fig. 4 and **Supplementary Fig. 4**). The genes for the different types (Type I-A, I-B, II-A, II-B, II-C and II-D) of *CHS* tended to map in the same chromosome region and gene clusters were found suggesting that they may have evolved via gene duplications, which in some cases may have been in tandem but in others, gene translocation within the same chromosome occurred. In general, chromosome organization for the *CHS* gene was conserved across the three species genomes and the *CHS* gene composition of MgiCh7, McoLG14 and MgaLG14, which contained members of *CHS* type IIA1 and IIA2 was identical. Moreover, gene mapping between the two Mytilidae species was also highly conserved suggesting that the evolutionary events that originated and established the *CHS* genes in bivalve genomes occurred before the Mytilidae and Ostreidae lineages diverged.

3.3. Expression of chitin-synthase

In *M. gigas*, the digestive gland and mantle expressed the highest number (20 isoforms) of *CHS*, followed by the gonads (19 *CHS* isoforms), and then the muscle and gills (14 *CHS* isoforms). Haemocytes expressed only 10 *CHS* isoforms, which was the lowest diversity observed. However, this expression trend differed in *M. galloprovincialis*, haemocytes (19 isoforms) = gills (19 isoforms) > mantle (16 isoforms) = muscles (16 isoforms) > digestive gland (12 isoforms) > gonads (7 isoforms) and *M. coruscus*, mantle (16 isoforms) > gills (13 isoforms) > gonads (6 isoforms) (Fig. 5). The genes *MgiChs-IIA1_5*, *MgiChs-IIC1*,

Table 1
Identification of *CHS* isoforms in the species of mollusc analyzed in the study.

SPECIES	Type I		Type II					
	Type I-A	Type I-B	Type II-A		Type II-B	Type II-C		Type II-D
			Type II-A-1	Type II-A-2		Type II-C-1	Type II-C-2	
Gymnomenia pellucida	-	1	-	-	1	1	1	-
Scutopus ventrolineatus	1	-	1	-	-	1	1	-
Acanthochitona crinita	-	3	-	-	1	1	1	-
Gadila tolmiei	1	2	1	-	1	1	-	1
Laevipilina hyalina	1	-	1	1	-	1	1	1
Octopus bimaculoides	1	5	2	-	1	-	1	1
Octopus sinensis	1	5	2	1	1	-	1	1
Lottia gigantea	-	-	3	1	1	1	2	1
Pomacea canaliculata	2	3	2	1	1	-	2	1
Aplysia californica	-	1	2	1	1	1	1	1
Biomphalaria glabrata	1	2	1	1	1	-	1	1
Mytilus coruscus	1	2	9	1	2	1	3	3
Mytilus galloprocincialis	1	3	7	1	2	1	3	3
Pecten maximus	2	1	1	1	1	1	2	3
Mizuhopeten yessoensis	2	1	1	1	1	1	2	3
Crassostrea virginica	1	1	7	1	3	1	1	2
Magallana gigas	3	2	6	1	2	1	2	5

Note: Graded colours from blue (1 isoform) to red (2 > isoforms) indicate the number of isoforms attributed to each species.

MgaChs-IB_1, and *MgaChs-IIA1_4* was not expressed in biomineralization-related tissues such as haemocytes and the mantle. Only data for the mantle was available for *M. coruscus* and revealed, *McoChs-IB_1*, *McoChs-IIA1_4*, *McoChs-IIA1_6*, *McoChs-IIA1_8*, *McoChs-IIA2*, and *McoChs-IIC1* were not expressed. *MgiChs-IID_2*, *MgaChs-IIC2_3*, and *McoChs-IID_3* was the most abundantly expressed isoforms, in the biomineralization tissues of *M. gigas*, *M. galloprovincialis*, and *M. coruscus*, respectively (Fig. 5A).

In *M. gigas*, *MgiChs-IID_5* was not expressed in pre- and post-shell formation larvae (Fig. 5B). The expression levels of *MgiChs-IB_1*, *MgiChs-IIA1_3*, and *MgiChs-IIC1* were significantly downregulated during shell formation, while the expression levels of *MgiChs-IB_2*, *MgiChs-IIA1_2*, *MgiChs-IIA1_5*, *MgiChs-IIA1_6*, *MgiChs-IIA2*, *MgiChs-IIB_2*, *MgiChs-IID_1*, and *MgiChs-IID_2* were significantly upregulated. In *M. galloprovincialis*, the expression levels of *MgaChs-IB_3*, *MgaChs-IIA1_2*, *MgaChs-IIA1_7*, and *MgaChs-IID_1* were significantly downregulated during shell formation, while the expression levels of *MgaChs-IB_2*, *MgaChs-IIA1_6*, *MgaChs-IIA2*, *MgaChs-IIB_1*, *MgaChs-IIC1*, *MgaChs-IIC2_1*, *MgaChs-IIC2_3*, and *MgaChs-IID_2* were significantly upregulated. In *M. coruscus*, *McoChs-IIA1_1* was not expressed in pre- and post-shell formation larvae, while the expression levels of *McoChs-IB_1*, *McoChs-IB_2*, *McoChs-IIA1_3*, *McoChs-IIA1_8*, *McoChs-IIA1_9*, *McoChs-IIA2*, *McoChs-IIB_1*, *McoChs-IIC2_1*, *McoChs-IIC2_2*, *McoChs-IIC2_3*, *McoChs-IID_1*, and *McoChs-IID_3* were significantly upregulated (Fig. 5B).

Under OA conditions, the expression levels of *MgaChs-IB_2*, *MgaChs-IID_2*, *McoChs-IB_2*, and *McoChs-IID_3* significantly decreased, while the expression levels of *MgaChs-IIA1_5*, *MgaChs-IIB_2*, *McoChs-IIA1_2*, *McoChs-IIA1_7*, and *McoChs-IIB_2* significantly increased. None of the CHS isoforms in *M. gigas* responded to 60 days of exposure to acidified seawater (Fig. 5C).

Taking into account the distribution of *CHS* in biomineralization-related tissues and their changing expression in larvae during shell formation, a total of 9 (*MgiChs-IB_1*, *MgiChs-IB_2*, *MgiChs-IIA1_1*, *MgiChs-IIA1_3*, *MgiChs-IIA1_6*, *MgiChs-IIA2*, *MgiChs-IIB_2*, *MgiChs-IID_1*, and *MgiChs-IID_2*), 12 (*MgaChs-IB_2*, *MgaChs-IB_3*, *MgaChs-IIA1_2*, *MgaChs-IIA1_6*, *MgaChs-IIA1_7*, *MgaChs-IIA2*, *MgaChs-IIB_1*, *MgaChs-IIC1*, *MgaChs-IIC2_1*, *MgaChs-IIC2_3*, *MgaChs-IID_1*, and *MgaChs-IID_2*), and 9 (*McoChs-IB_2*, *McoChs-IIA1_3*, *McoChs-IIA1_9*, *McoChs-IIB_1*, *McoChs-IIC2_1*, *McoChs-IIC2_2*, *McoChs-IIC2_3*, *McoChs-IID_1*, and *McoChs-IID_3*) *CHS* isoforms were categorized as being related to shell biomineralization in the three species. Cross referencing of the *CHS* isoforms identified in tissues related to biomineralization (mantle and haemocytes) and biomineralizing larvae with those that changed under an OA challenge identified a small number of common isoforms *MgaChs-IB_2*, MgaChs-IID_2, *McoChs-IB_2*, and *McoChs-IID_3* in the genus *Mytilus* that were tentatively assigned a function-related classification, namely, shell formation-related genes influenced by OA. Expression levels of *CHS* isoforms identified in transcriptome analysis (unpublished) to have a significant response to OA in *M. galloprovincialis* were further analysed by qPCR (Fig. 6) and revealed the expression profile was similar between the NGS tag counts (RFMPK) and qPCR analysis.

4. Discussion

4.1. Mytilidae and Ostreidae have the biggest CHS gene family expansion in studied eukaryotes

CHS enzymes are involved in chitin synthesis an important element of the shell organic matrix in Mollusca and so these enzymes have long been the focus of work about mollusc biomineralization (Han et al., 2016; Peng et al., 2023; Schönitzer and Weiss, 2007; Sengupta Ghatak et al., 2013; Suzuki et al., 2007; Weiss, 2012). However, the evolution of CHS in molluscs is surprisingly poorly studied even though substantial genomic and transcriptomic resources are now publicly available particularly those of commercially importance Mollusca such as Cephalopoda, Gastropoda, and Bivalvia (Gomes-dos-Santos et al., 2020; Takeuchi, 2017). To comprehensively describe the evolution of *CHS* in Mollusca, we analysed *CHS* isoforms in genome data from as many species as possible. For the classes Cephalopoda, Gastropoda, and Bivalvia multiple species were analysed and multiple genes encoding *CHS* isoforms were retrieved but for other Mollusca taxonomic classes a single representative species was used. Previous studies proposed that

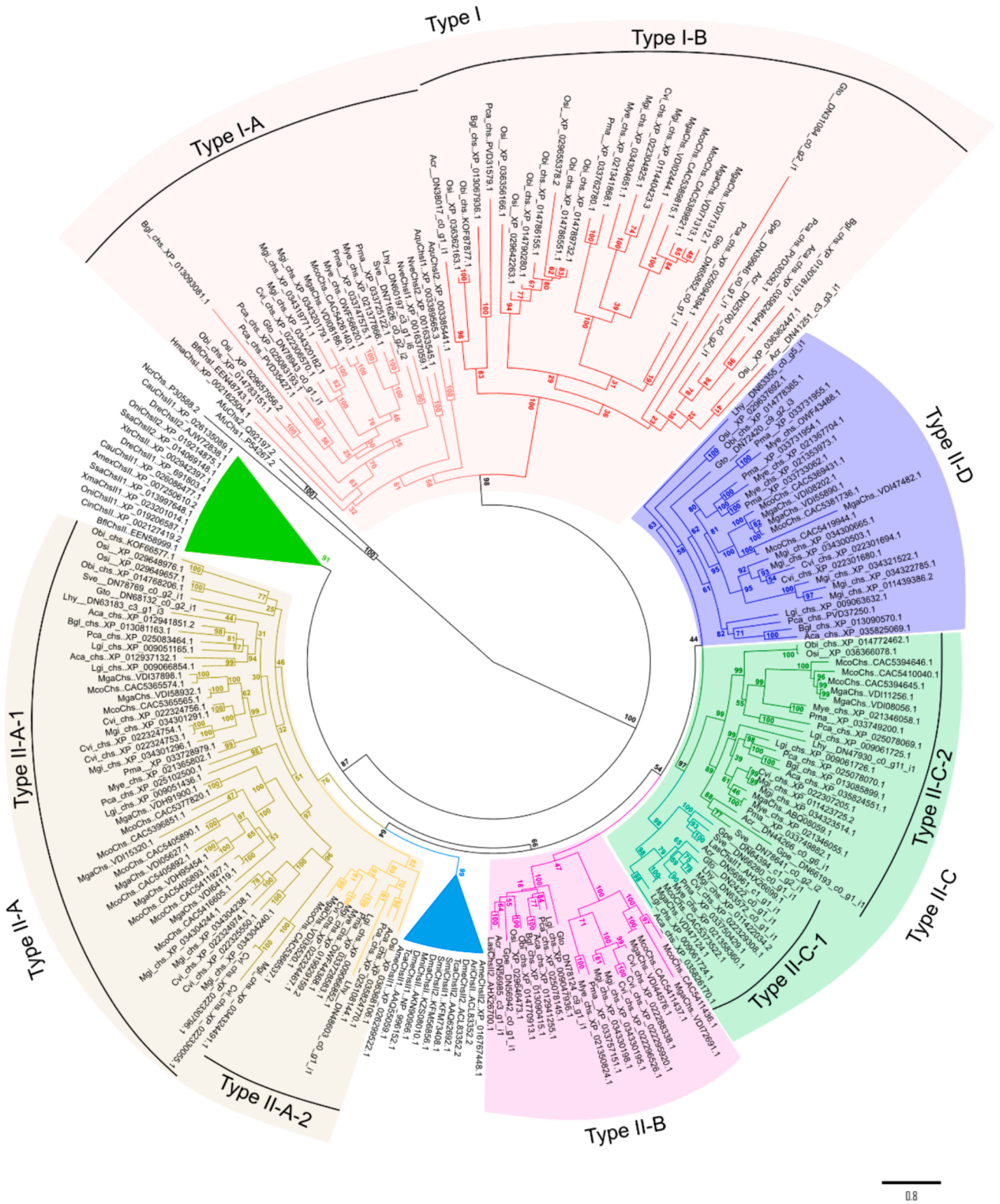

Fig. 2. Phylogenetic analysis of mollusc, arthropod and chordate chitin-synthases. The Maximum Likelihood method was used to build the illustrated tree and a tree with a similar topology was obtained when the BI method was utilised and is available in **Supplementary Fig. 1**. The ML tree was built in PhyML 3.0 from the ATGC bioinformatics platform (http://www.atgc-montpellier.fr/phyml/) using SMS automatic model selection for the study of protein evolution according to AIC (Akaike Information Criterion) with 1000 bootstrap replicates for the node branches. The accession numbers and name given to the sequences used are in **Supplementary Table 1**. The clade without a coloured background represents the Fungi *CHS* gene isoforms and was used to root the tree. The members within the chordate and arthropod clades were merged and are represented in green and blue, respectively. "*" indicates the cephalochordate *B. floridae* sequences that cluster within CHS Type I and Type II.

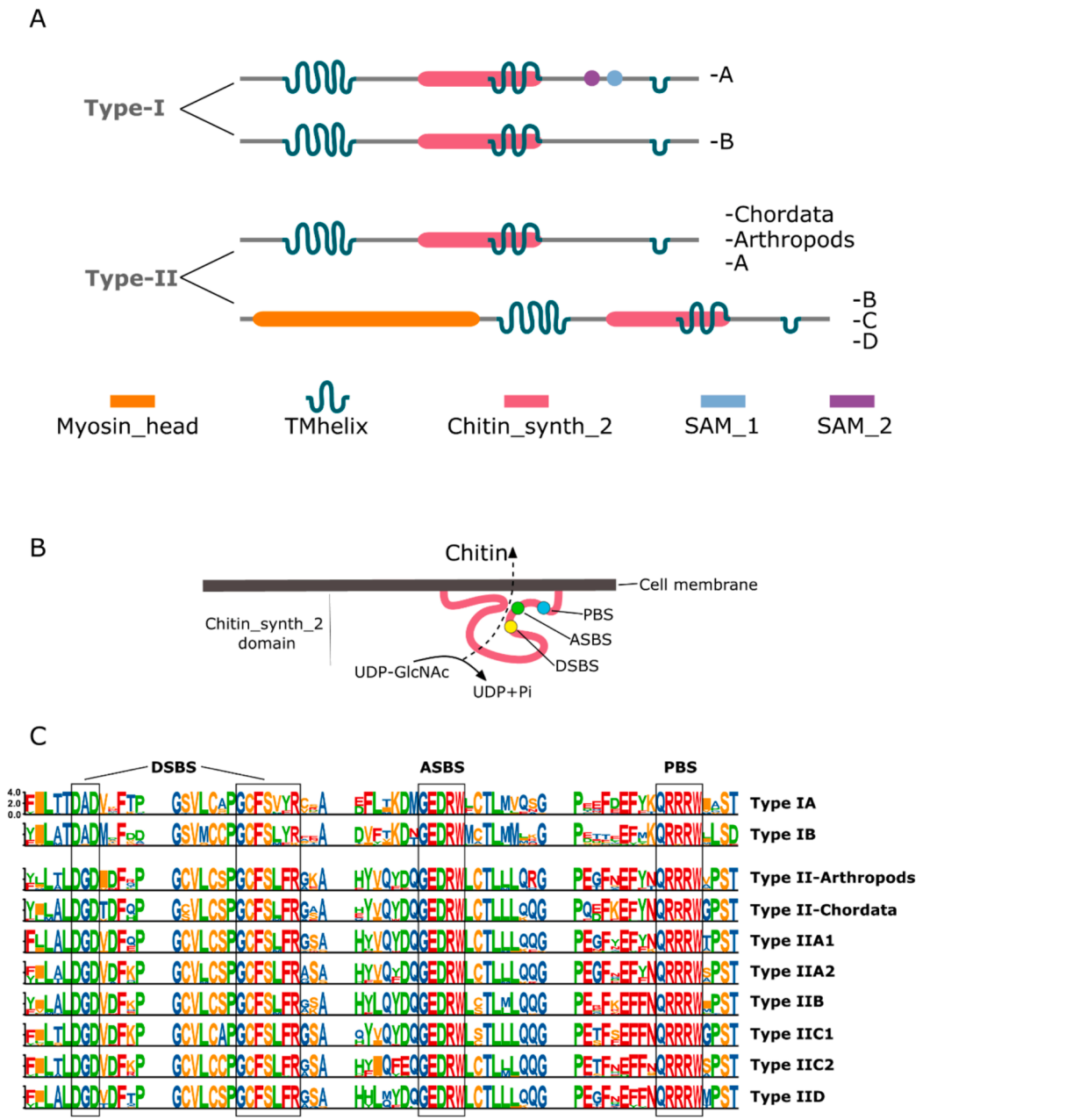

Fig. 3. Schematic representation of the A) deduced protein structure of the CHS isoforms, B) representation of the catalytic center of the Chitin_synth_2 domain, and C) multiple sequence alignment of the CHS catalytic center (Chitin-synth_2) in metazoans. A) Linear representation of the domains predicted by Pfam for the different types of CHS. CHS proteins that uniquely possess a Chitin_synth_2 domain (indicated in pink) and transmembrane regions (indicated in turquoise). The presence or absence of a Myosin_head (indicated in orange), sterile alpha motif 1 (SAM_1, blue) and SAM_2 (purple) domains are isoform specific. B) Schematic representation of the catalytic center of the Chitin_synth_2 domain, identified by (Weiss, 2012), and the functional motifs, donor saccharide binding site (DSBS), acceptor saccharide binding site (ASBS) and product binding site (PBS), are indicated. C) Multiple sequence alignment of the functional motifs of the catalytic center present in the Chitin_synth_2 domain. Sequence gaps were introduced to facilitate visualization of the functional domains (for the full sequence alignment containing all collected sequences see **Supplementary Fig. 3**). Amino acids were colored using the MSA default settings and the height of letters are indicative of amino acid residue conservation across multiple sequences (the bigger the letter, the higher the sequence conservation). (For interpretation of the references to colour in this figure legend, the reader is referred to the web version of this article.)

the *CHS* family was expanded in the phylum Mollusca, and the gastropod *L. gigantea* was suggested to have the highest number of *CHS* gene isoforms (10) in its genome. Recently, Shi et al. (2020) conducted a thorough reannotation of the genome data of amphioxus species and identified 11–12 *CHS* isoforms including previously unidentified *CHS* genes (Shi et al., 2020).

Based on sequence alignments and Chitin_synth_2 domain analysis, we conducted an in-depth exploration of the genomes of 17 mollusc species. This revealed that bivalves, in particular, the order Mytilidae (~22 isoforms), and Ostreidae (~17–22 isoforms), underwent the most extensive gene family expansion of the eukaryotes analysed to date (Fig. 7). Genome analysis in molluscs suggests *CHS* gene family expansion occurred by gene/genome duplication events before the Mytilidae and Ostreidae divergence.

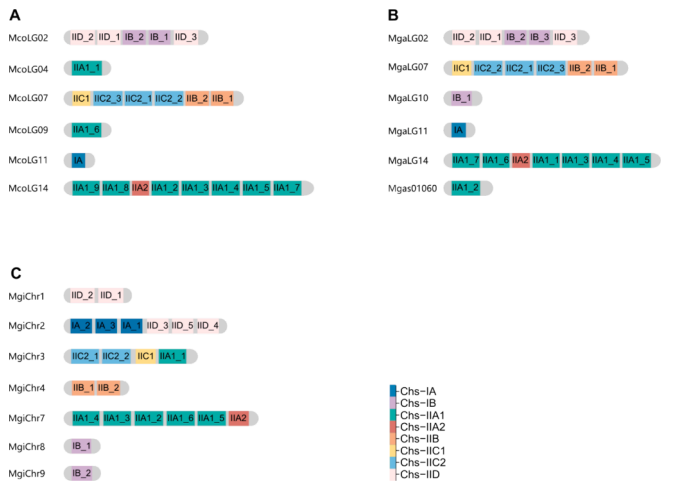

Fig. 4. Mapping of the CHS genes in the genomes of the three bivalves: A) *M. coruscus* (Mco), B) *M. galloprovincialis* (Mga) and C) *M. gigas* (Mgi). CHS genes were mapped against the most recent genome assemblies at the chromosome level available for the three species (for the details of mapping see **Supplementary Fig. 4**). The chromosome names for each species are indicated and the gene names are identified and the CHS isoforms are coloured by type.

4.2. CHS have a complex evolutionary history and further differentiation may have arisen in the last common ancestor of molluscs

CHS is widespread among eukaryotes and has a complex evolutionary history (Roncero, 2002). Independently formed paralogous groups are an important feature in the evolutionary history of *CHS*. According to Morozov and Likhoshway's (2016) the evolution of *CHS* in eukaryotes can be divided into two main branches, with metazoan *CHS* forming one branch (Morozov and Likhoshway, 2016). Previous phylogenetic analysis revealed most fungi have several different *CHS* genes and that fungal *CHS* form seven monophyletic classes within two divisions (Roncero, 2002; Ruiz-Herrera and Ruiz-Medrano, 2004). The results of the present study were consistent with previous studies since metazoan *CHS* clustered in two branches (Type I and Type II), and Porifera and Cnidaria *CHS* isoforms were restricted to Type I, while Arthropod *CHS* isoforms were clustered together in the Type II branch (Shi et al., 2020; Zakrzewski et al., 2014). The identification of Type I *CHS* in amphioxus but its absence in most Chordates has been taken to suggest that Type I *CHS* was lost in this lineage (Guerriero, 2012; Shi et al., 2020). Furthermore, like in the chordates the Arthropods were also proposed to have lost Type I *CHS* (Merzendorfer, 2011, 2006). Nonetheless, in the molluscs both Type I and Type II *CHS* genes were retained and underwent a significant expansion. Since all four branches (*CHS* Type II A-D) in the phylogenetic tree generated contained sequences from different lophotrochozoan animals (i.e., Mollusc, Brachiopods, Entoprocts, and Annelids) as found in previous evolutionary studies (Choi et al., 2022; Edgecombe et al., 2011; Helmkampf et al., 2008), we hypothesis that four type II *CHS* clusters already existed in the last common ancestor of the lophotrochozoans, which is in line with previous reports (Zakrzewski et al., 2014). The present study raises a straightforward hypothesis to explain the results obtained, namely that the last ancestor of molluscs may have further expanded Type I, Type II A, and Type II C genes and this was subsequently followed by varying degrees of *CHS* gene loss in the different lineages (Fig. 8). The gene loss occurred in bivalves with and without a biomineralized shell suggesting that *CHS* may have other biological roles in addition to shell formation. Curiously, no *CHS* type II-D was identified in members of the shell-less Aplacophoran and multi-shelled Polyplacophoran Molluscs (*Gymnomenia pellucida, Scutopus ventrolineatus and Acanthochitona crinite*). It is hypothesised that the emergence of the type II-D isoform may be related to the appearance of Conchifera Mollusca, but this remains to be established when more data on representatives of the Aculifera subphylum becomes available (Fig. 8).

4.3. Chitin synthesized by CHS may not only be involved in shell formation in molluscs

In Porifera and Cnidaria, that possess only Type I CHS, most species have a mineralized exoskeleton, and this led to the proposal that Type I CHS is essential for the shell and synthesizes chitin (Bo et al., 2012; Ehrlich et al., 2007; Zakrzewski et al., 2014). The premise that chitin is synthesized only for exoskeleton formation in Porifera and Cnidaria has yet to be confirmed. Furthermore, recent research by (Vandepas et al., 2023) on the tissue distribution and expression of *CHS* genes in a Cnidaria that lacks a hard exoskeleton, indicated chitin probably has several functions in its biology. A role for chitin in more than the formation of a mineralized shell would explain why CHS is found in vertebrates and soft-bodied molluscs (such as *Aplysia californica*).

Current research into the function of mollusc CHS has focused on its role in shell biomineralization (Schönitzer and Weiss, 2007; Sengupta Ghatak et al., 2013; Suzuki et al., 2007; Weiss, 2012). However, the identification of CHS in nonmineralized tissues and in larvae without a developed shell in the present study is indicative of a much broader biological role for *CHS* isoforms that may be uncovered by closer scrutiny of the potential functions of chitin. There are relatively few reports that explicitly define the function of different *CHS* isoforms, although (Weiss et al., 2006) reported that the Type II *CHS* isoform containing a myosin head (corresponding to *MgaChs-IIC2_3* in this study) have a role in shell formation. Although results in *Tegillarca granosa* are contradictory since in this species Type II *CHS* isoforms regulate polyspermy, and blockade of enzyme activity in oocytes significantly increased polyspermy (Han et al., 2016).

4.4. Conserved domain differentiation in Mollusca CHS isoforms is independent of shell emergence

The myosin head domain, in CHS, may be one of the core functional domains for shell formation in metazoans (Weiss, 2012). The presence of a complex transmembrane structure and myosin head domain in CHS suggests it may regulate the cellular cytoskeleton and membrane biophysics during assembly of organic matrices (Burridge and Wennerberg, 2004; Weiss et al., 2013). This is corroborated by studies of oomycete CHS, which has domains for interaction with microtubules and trafficking in the N-terminal region (Guerriero et al., 2010). The evolutionary origin of the myosin head domain in fungal CHS and in some lophotrochozoan CHS isoforms is intriguing. Analysis of CHS in fungi and lophotrochozoans from a "myosin-head" perspective suggests that at least two independent fusion events occurred, that resulted in highly similar outcomes (Zakrzewski et al., 2014), and that a third independent fusion event may have occurred in diatoms that also have CHS with a myosin head domain (Durkin et al., 2009). Furthermore, the results of the present study make it clear that the myosin head domain is not fully preserved in molluscs within Type II (B-D groups) CHS and this presumably has functional consequences. The loss events associated with CHS may be indicative of functional differentiation.

The Chitin_synth_2 domain is a well conserved structural domain characteristic of metazoan CHS, along with the complex N- and C-terminal transmembrane domains. The catalytic center of the Chitin_synth_2 domain contains three highly conserved functional motifs in the intracellular region (Fig. 3). In the present study the donor saccharide binding site was the most notable difference between Type I and Type II CHS in the conserved domain sequence. Although if this structural difference is reflected in functional differentiation of CHS isoforms was not demonstrated. Furthermore, the Type I-A CHS isoform also contains a SAM domain, which is believed to play an important role in protein–protein interactions (Thanos et al., 1999). Taken together the proceeding observations imply functional differentiation occurs

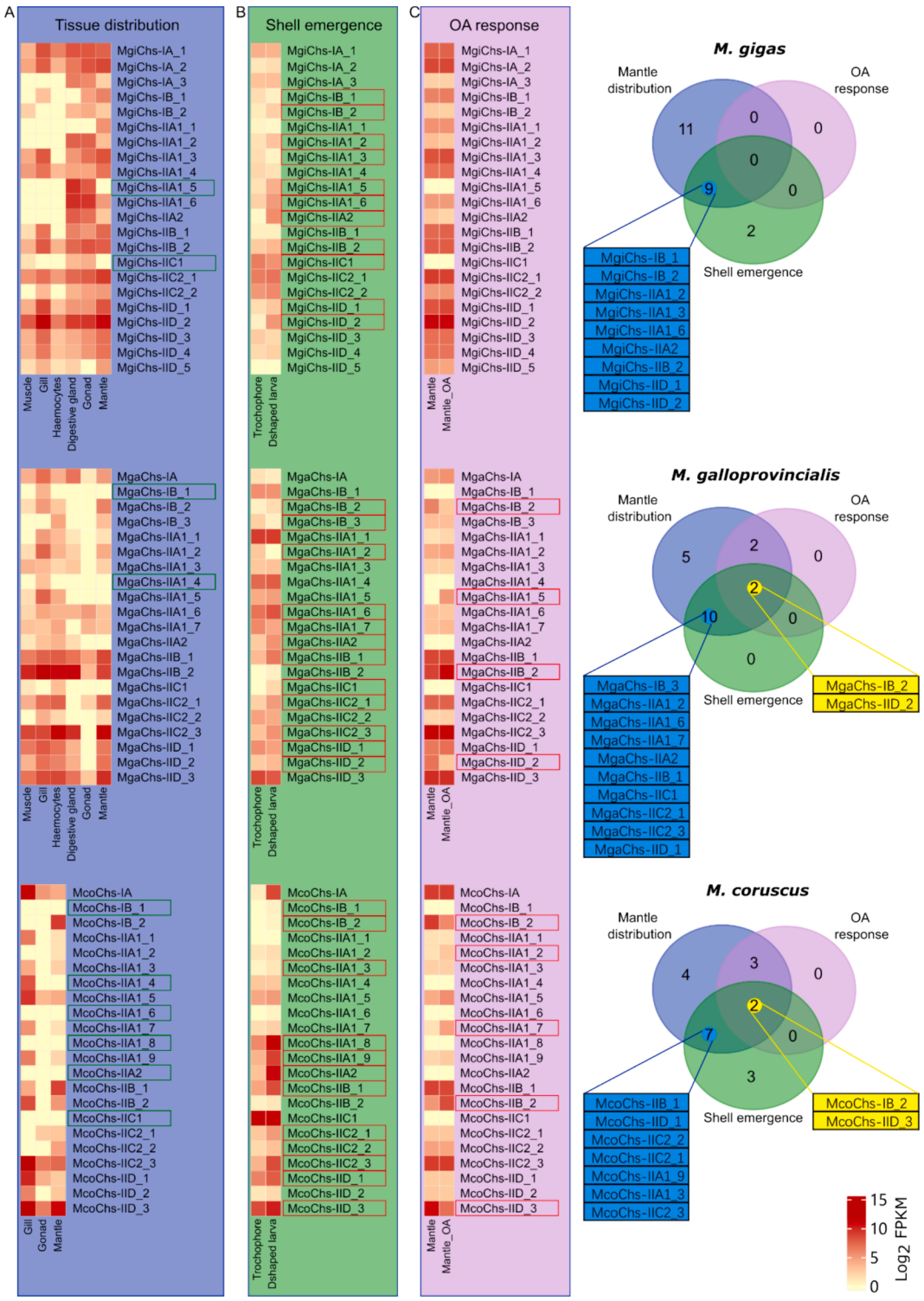

Fig. 5. Heatmap of *CHS* expression in tissues (A), during larval biomineralization, (B) and in the mantle of bivalves exposed to OA conditions (C) in three species. Graded colours from yellow (low) to red (high) indicate the relative expression abundance of each *CHS* gene isoform. In A) the green boxes represent the *CHS* isoforms that are not expressed in the mantle and haemocytes (tissues involved in shell formation), B) represents *CHS* isoform expression before (Trochophore, without shell) and after (D-shaped larva) shell appearance during the bivalve larval life cycle and the red boxes indicate the isoforms that were significantly (up or downregulated), C) represents the *CHS* isoform response in the mantle under OA and the red boxes indicate the *CHS* isoforms that significantly responded (up or downregulated) to OA exposure. The Venn diagram shows the *CHS* isoforms identified using the following criteria: 1) Expressed in shell formation related tissues (mantle and haemocytes), 2) Changes significantly after OA exposure, 3) Changes significantly during larval shell development. Candidate *CHS* genes likely to be involved in bivalve shell formation are marked in blue and the genes in yellow are the candidate bivalve shell forming *CHS* isoforms that responded to OA. (For interpretation of the references to colour in this figure legend, the reader is referred to the web version of this article.)

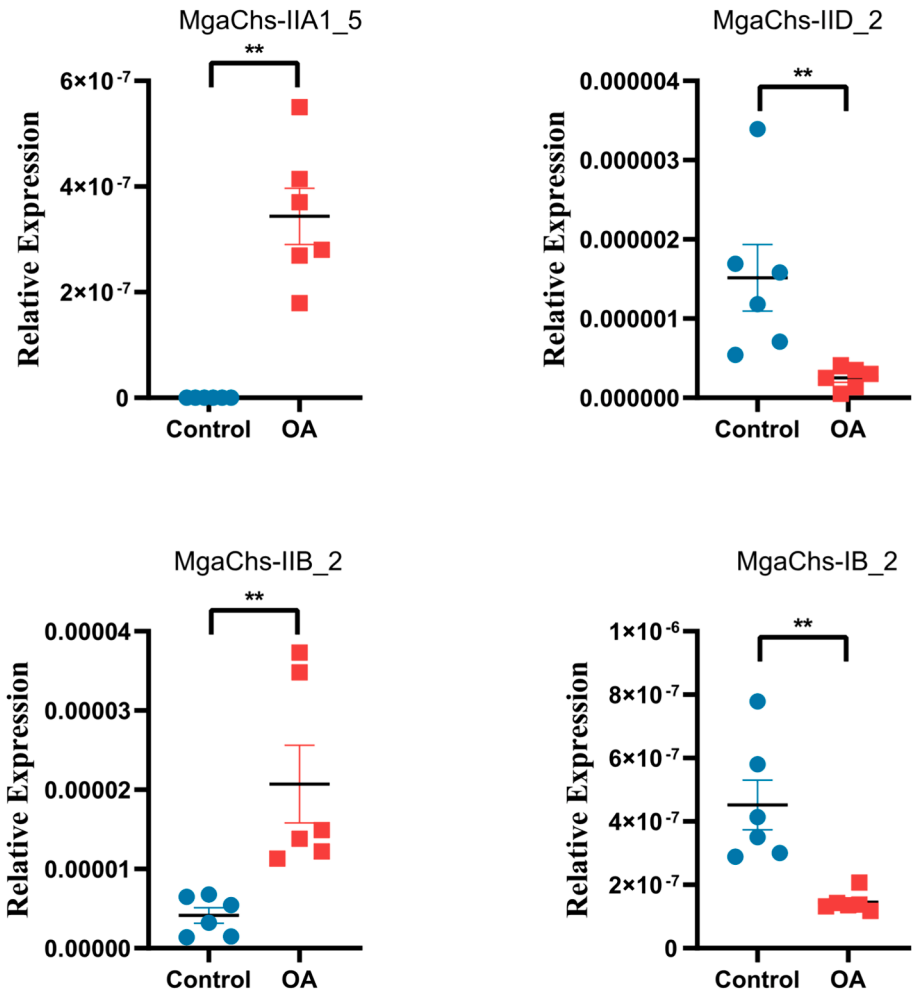

Fig. 6. Analysis by qPCR of *CHS* isoforms with a significantly different expression in *M. galloprovincialis* mantle maintained in normal seawater and OA seawater. *CHS* isoforms selected for analysis were obtained from a transcriptome study (Peng et al., unpublished). The relative expression of *CHS* isoforms in the mantle of *M. galloprovincialis* exposed to normal and OA seawater was determined by normalizing the gene expression by the average of the expression of two reference genes that did not vary under experimental conditions (*EF1α* and *18S*). Statistical analysis was performed for the qPCR results using a t-test and the data represent the mean ± SEM of n = 6 biological replicates. Asterisks indicate significantly different groups at $p < 0.05$.

between Type I-A and Type I-B CHS isoforms and potentially in chitin production.

4.5. *The influence of extracellular pH on the enzyme activities of different CHS isoform is species-specific*

The extracellular portion of CHS sequences has a significant impact on function since it has a crucial role in chitin polymerization (Yabe et al., 1998). This is surprising considering the lower sequence conservation of the extracellular portion of CHS identified in the present study. (Weiss et al., 2013) identified in *Atrina rigida* CHS (*Ar-CS1*) an extracellular domain important for chitin assembly, that might regulate chitin synthesis and myosin movements, which are thought to be important for shell formation. It has been proposed that at appropriate extrapallial pH conditions transmembrane supramolecular arrays may form of myosin CHSs stabilized by their extracellular domain and that these structures may be involved in the regulation of mollusc shell architecture (Weiss, 2012). Interestingly OA in *M. galloprovincialis* modified the expression of *CHS* isoforms that lack the myosin head domain, suggesting in common with *A. rigida* extracellular pH influenced its expression and this effect was not related to the theoretical pI of the CHS protein (**Supplementary Table 4**).

Our results not only support the species-specific response of CHS to OA but also suggest a broad impact of reduced seawater pH on multiple CHS isoforms in *Mytilus*. Four and five genes showed modified expression in *M. galloprovincialis* and *M. coruscus*, respectively and only the mytilid *Chs-IB_2* and *Chs-IIB_2* sequence orthologues had a similar expression pattern. The other transcript sequence orthologues did not, which seems to run counter to the general principle that gene orthologues have equivalent function in different organisms (Gabaldón and Koonin, 2013). Considering the structure of the deduced CHS protein we would propose that enzyme activity (function) is most likely conserved between bivalves. However, the divergent expression patterns of *CHS* gene orthologues under reduced seawater pH (OA) in our study may not reflect differences in function but rather differences in animal physiology and capacity to cope across time. Further work will be required to better characterise *CHS* gene orthologues.

This contrasts with the situation in *M. gigas* larvae where only two *CHS* isoforms were reported to be significantly regulated under OA (Zhang et al., 2019). The different response observed in *M. gigas* larvae and adults is unsurprising as they also have a significantly different response to OA (Gazeau et al., 2013). The more limited nutrient resources for energy metabolism in larvae has been proposed to explain their higher susceptibility to the effects of OA (Gazeau et al., 2013; Tan and Zheng, 2020). Our studies on the molecular processes in the mantle under OA indicate that *M. galloprovincialis* and *M. gigas* respond differently (Peng et al., unpublished) and it was proposed that shell type (calcite or aragonite), which have a different metabolic cost for

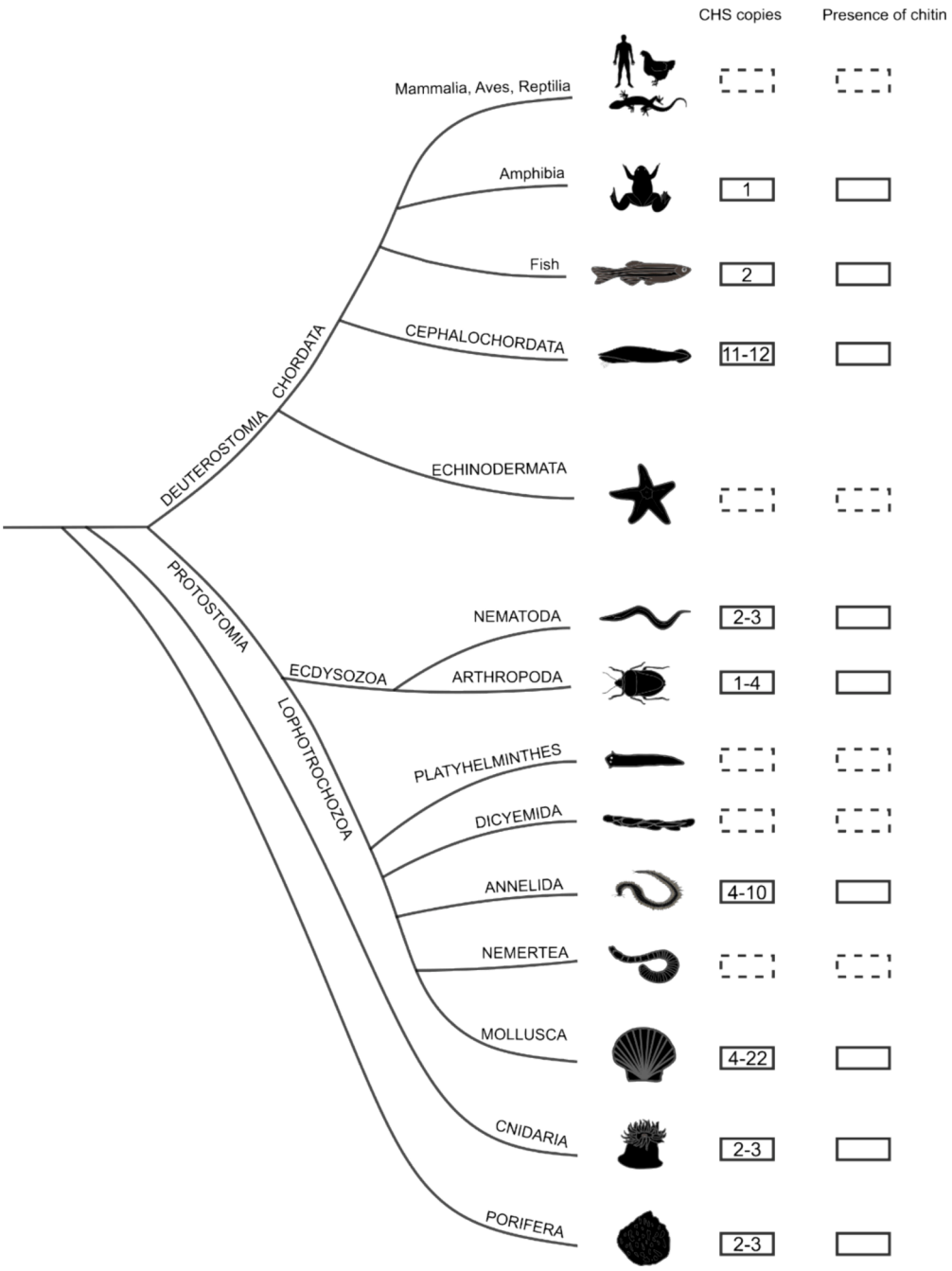

Fig. 7. A diagrammatic representation of the distribution of the *CHS* isoforms and the polysaccharide chitin in metazoan. The inferred evolutionary tree is obtained from Peng et al., (2022). The dashed boxes indicate absence of *CHS* or that chitin has not been documented, and the number in the solid boxes indicates the minimum and maximum numbers of *CHS* isoforms possessed by species at the taxonomic level. The nr database (https://ftp.ncbi.nlm.nih.gov/blast/db/FASTA/) was used to identify species *CHS* homolog copy numbers. All mollusc species contain chitin, which is found in shells, beaks, sucker discs, radula and oesophageal cuticles.

construction determine their response (Clements et al., 2017; Lassoued et al., 2019). The bigger suite of biomineralization toolbox genes and energy-related and regulatory-related gene transcripts in mantle transcriptomes of *M. galloprovincialis* exposed to OA may explain their greater capacity to regulate biomineralization toolbox genes and may explain their reduced growth as energy is diverted to the more costly process of building aragonite crystals and packing them into a regular arrangement (Peng et al., unpublished). Considering the species-specificity of *CHS* tissue distribution, in larval shell formation, and in OA identified in the present study, we speculate that the response of *CHS* in the mantle to OA is likely to be related to shell growth and maintenance and that *CHS* Type I-B and Type II-D in *Mytilus* are the isoforms involved. The modifications observed in the expression of other *CHS* gene isoforms is proposed to be related to other biological functions.

5. Conclusion

In this study, the evolution of *CHS* gene isoforms was comprehensively explored at the class level in molluscs and compared to *CHS* in members of other phyla. Analysis of available genomes revealed that bivalves have the highest number of *CHS* gene isoforms of all eukaryotes. This study corroborates and supports the proposal that all four branches of *CHS* Type II (A-D) in lophotrochozoan animals existed in their last common ancestor (Zakrzewski et al., 2014). Moreover, we

CLASSES	Type I		Type II					
	Type I-A	Type I-B	Type II-A		Type II-B	Type II-C		Type II-D
			Type II-A-1	Type II-A-2		Type II-C-1	Type II-C-2	
Solenogastres	-	•	-	-	•	•	•	-
Caudofoveata	•	-	•	-	-	•	•	-
Polyplacophora	-	•	-	-	•	•	•	-
Scaphopoda	•	•	•	-	•	•	-	•
Monoplacophora	•	-	•	•	-	•	•	•
Cephalopoda	•	•	•	•	•	-	•	•
Gastropoda	•	•	•	•	•	•	•	•
Bivalvia	•	•	•	•	•	•	•	•

Fig. 8. Evolution of *CHS* genes in Mollusca. The green shaded boxes with a dash and un-shaded boxes with a dot indicate *CHS* isoform loss and presence, respectively. (For interpretation of the references to colour in this figure legend, the reader is referred to the web version of this article.)

further confirmed that *CHS* type II in the last common ancestor of molluscs diverged and gave rise to Type II-A and Type II-C clades. At the class level in Mollusca, isoform loss was variable, and such losses were unrelated to the presence of a mineralized shell indicating a much wider functional role for CHS.

Differences in the donor saccharide binding site at the catalytic centre of the chitin_synth_2 domain in Type I and Type II CHS is strongly indicative of functional differentiation between these two major isoforms. The myosin head domain was not conserved in all Type II (B-D groups) CHS in molluscs, even in isoforms of functional importance in shell formation. Additionally, pronounced species-specific tissue distributions of *CHS* isoforms, strongly suggests that functional diversification or involvement in functions beyond shell biomineralization exist. By screening transcriptome data from larvae before and after shell formation it was possible to identify *CHS* isoforms with a concordant expression pattern with mineralization-related genes and these isoforms were putatively assigned a role in shell formation. There are three different chitin allomorph types (α, β, and γ) found in nature and in Mollusca shells β-chitin is the predominant form (Karthick Rajan et al., 2024). However, considering the large diversity of *CHS* isoforms and their ubiquitous tissue distribution it seems likely that the other types of chitins have other biological functions other than shell formation.

CRediT authorship contribution statement

Maoxiao Peng: Writing – original draft, Visualization, Software, Methodology, Investigation, Formal analysis, Data curation, Conceptualization. **João C.R. Cardoso:** Writing – review & editing, Writing – original draft, Validation, Supervision, Project administration, Investigation, Funding acquisition, Formal analysis. **Deborah M. Power:** Writing – review & editing, Supervision, Project administration, Funding acquisition.

Data availability

Data will be made available on request.

Acknowledgments

This study received Portuguese national funds from FCT - Foundation for Science and Technology through project UIDB/04326/2020 (DOI:10.54499/UIDB/04326/2020), UIDP/04326/2020 (DOI:10.54499/UIDP/04326/2020) and LA/P/0101/2020 (DOI:10.54499/LA/P/0101/2020), and from the operational programmes CRESC Algarve 2020 and COMPETE 2020 through projects EMBRC.PT ALG-01-0145-FEDER-022121 and BIODATA.PT ALG-01-0145-FEDER-022231.

Appendix A. Supplementary material

Supplementary data to this article can be found online at https://doi.org/10.1016/j.ympev.2024.108192.

References

Bo, M., Bavestrello, G., Kurek, D., Paasch, S., Brunner, E., Born, R., Galli, R., Stelling, A. L., Sivkov, V.N., Petrova, O.V., 2012. Isolation and identification of chitin in the black coral *Parantipathes larix* (Anthozoa: Cnidaria). Int. J. Biol. Macromol. 51, 129–137.
Burridge, K., Wennerberg, K., 2004. Rho and Rac take center stage. Cell 116, 167–179.
Chan, V.B.S., Johnstone, M.B., Wheeler, A.P., Mount, A.S., 2018. Chitin facilitated mineralization in the eastern oyster. Front. Mar. Sci. 5, 347.
Chen, C., Chen, H., Zhang, Y., Thomas, H.R., Frank, M.H., He, Y., Xia, R., 2020. TBtools: an integrative toolkit developed for interactive analyses of big biological data. Mol. Plant 13, 1194–1202.
Choi, H., Kim, S.L., Jeong, M.K., Yu, O.H., Eyun, S., 2022. Identification and phylogenetic analysis of chitin synthase genes from the deep-sea polychaete Branchipolynoe onnuriensis genome. J. Marine Sci. Eng. 10 (5), 598.
Clements, J.C., Bourque, D., McLaughlin, J., Stephenson, M., Comeau, L.A., 2017. Extreme ocean acidification reduces the susceptibility of eastern oyster shells to a polydorid parasite. J. Fish Dis. 40, 1573–1585.
Desbrières, J., Guibal, E., 2018. Chitosan for wastewater treatment. Polym. Int. 67, 7–14.
Durkin, C.A., Mock, T., Armbrust, E.V., 2009. Chitin in diatoms and its association with the cell wall. Eukaryot. Cell 8, 1038–1050.
Edgar, R.C., 2004. MUSCLE: multiple sequence alignment with high accuracy and high throughput. Nucleic Acids Res. 32, 1792–1797.
Edgecombe, G.D., Giribet, G., Dunn, C.W., Hejnol, A., Kristensen, R.M., Neves, R.C., Rouse, G.W., Worsaae, K., Sørensen, M.V., 2011. Higher-level metazoan relationships: recent progress and remaining questions. Org. Divers. Evol. 11, 151–172.
Ehrlich, H., Maldonado, M., Spindler, K., Eckert, C., Hanke, T., Born, R., Goebel, C., Simon, P., Heinemann, S., Worch, H., 2007. First evidence of chitin as a component of the skeletal fibers of marine sponges. Part I. Verongidae (Demospongia: Porifera). J. Exp. Zool. B Mol. Dev. Evol. 308, 347–356.
Emms, M.D., Kelly, S., 2019. OrthoFinder: phylogenetic orthology inference for comparative genomics. Genome Biol. 20, 1–14.
Falini, G., Fermani, S., 2004. Chitin mineralization. Tissue Eng. 10, 1–6.
Falini, G., Albeck, S., Weiner, S., Addadi, L., 1996. Control of aragonite or calcite polymorphism by mollusk shell macromolecules. Science 1979 (271), 67–69.
Furuhashi, T., Beran, A., Blazso, M., Czegeny, Z., Schwarzinger, C., Steiner, G., 2009. Pyrolysis GC/MS and IR spectroscopy in chitin analysis of molluscan shells. Biosci. Biotech. Bioch. 73, 93–103.
Gabaldón, T., Koonin, E.V., 2013. Functional and evolutionary implications of gene orthology. Nat. Rev. Genet. 14 (5), 360–366.
Gazeau, F., Parker, L.M., Comeau, S., Gattuso, J.-P., O'Connor, W.A., Martin, S., Pörtner, H.-O., Ross, P.M., 2013. Impacts of ocean acidification on marine shelled molluscs. Mar. Biol. 160, 2207–2245.
Gomes-dos-Santos, A., Lopes-Lima, M., Castro, L.F.C., Froufe, E., 2020. Molluscan genomics: the road so far and the way forward. Hydrobiologia 847, 1705–1726.
Gooday, G.W., 1999. Aggressive and defensive roles for chitinases. EXS 87, 157–169.
Guerriero, G., 2012. Putative chitin synthases from Branchiostoma floridae show extracellular matrix-related domains and mosaic structures. Genom. Proteom. Bioinform. 10, 197–207.

Guerriero, G., Avino, M., Zhou, Q., Fugelstad, J., Clergeot, P.-H., Bulone, V., 2010. Chitin synthases from Saprolegnia are involved in tip growth and represent a potential target for anti-oomycete drugs. PLoS Pathog. 6, e1001070.
Han, Y., Shi, W., Guo, C., Zhao, X., Liu, S., Wang, Y., Su, W., Zha, S., Wu, H., Chai, X., 2016. Characteristics of chitin synthase (CHS) gene and its function in polyspermy blocking in the blood clam Tegillarca granosa. J. Moll. Stud. 82, 550–557.
Helmkampf, M., Bruchhaus, I., Hausdorf, B., 2008. Phylogenomic analyses of lophophorates (brachiopods, phoronids and bryozoans) confirm the Lophotrochozoa concept. Proc. R. Soc. B Biol. Sci. 275, 1927–1933.
Heredia, A., Aguilar-Franco, M., Magaña, C., Flores, C., Piña, C., Velázquez, R., Schäffer, T.E., Bucio, L., Basiuk, V.A., 2007. Structure and interactions of calcite spherulites with α-chitin in the brown shrimp (*Penaeus aztecus*) shell. Mater. Sci. Eng. C 27, 8–13.
Hönisch, B., Ridgwell, A., Schmidt, D.N., Thomas, E., Gibbs, S.J., Sluijs, A., Zeebe, R., Kump, L., Martindale, R.C., Greene, S.E., 2012. The geological record of ocean acidification. Science 335 (6072), 1058–1063.
Karthick Rajan, D., Mohan, K., Rajarajeswaran, J., Divya, D., Kumar, R., Kandasamy, S., Zhang, S., Ramu Ganesan, A., 2024. β-Chitin and chitosan from waste shells of edible mollusks as a functional ingredient. Food Front 5, 46–72.
Kramer, K.J., Koga, D., 1986. Insect chitin: physical state, synthesis, degradation and metabolic regulation. Insect Biochem. 16, 851–877.
Lassoued, J., Babarro, J.M.F., Padín, X.A., Comeau, L.A., Bejaoui, N., Pérez, F.F., 2019. Behavioural and eco-physiological responses of the mussel *Mytilus galloprovincialis* to acidification and distinct feeding regimes. Mar. Ecol. Prog. Ser. 626, 97–108.
Marin, F., Le Roy, N., Marie, B., 2012. The formation and mineralization of mollusk shell. Front. Biosci.-Scholar 4, 1099–1125.
Merzendorfer, H., 2006. Insect chitin synthases: a review. J. Comp. Physiol. B 176, 1–15.
Merzendorfer, H., 2011. The cellular basis of chitin synthesis in fungi and insects: common principles and differences. Eur. J. Cell Biol. 90, 759–769.
Morozov, A.A., Likhoshway, Y.V., 2016. Evolutionary history of the chitin synthases of eukaryotes. Glycobiology 26, 635–639.
Muzzarelli, R.A.A., 2013. Chitin. Elsevier.
Peng, M., Cardoso, J.C.R., Pearson, G., Canário, A.V.M., Power, D.M., 2023. Core genes of biomineralization and cis-regulatory long non-coding RNA regulate shell growth in bivalves. J. Adv. Res.
Peng, M., Cardoso, C.R.J., Sorigué, P., Power, M.D., (unpublished). Species-specific responses of bivalves to ocean acidification.
Peng, M., Li, Z., Cardoso, J.C.R., Niu, D., Liu, X., Dong, Z., Li, J., Power, D.M., 2022. Domain-dependent evolution explains functional homology of protostome and deuterostome complement C3-like proteins. Front. Immunol. 13, 840861.
Roncero, C., 2002. The genetic complexity of chitin synthesis in fungi. Curr. Genet. 41, 367–378.
Ruiz-Herrera, J., Ruiz-Medrano, R., 2004. Chitin biosynthesis in fungi. In: Arora, D.K., Bridge, P.D., Bhatnagar, D. (Eds.), Handbook of Fungal Biotechnology. Marcel Dekker Inc., New York, pp. 315–330.
Schönitzer, V., Weiss, I.M., 2007. The structure of mollusc larval shells formed in the presence of the chitin synthase inhibitor Nikkomycin Z. BMC Struct. Biol. 7, 1–24.
Sengupta Ghatak, A., Koch, M., Guth, C., Weiss, I.M., 2013. Peptide induced crystallization of calcium carbonate on wrinkle patterned substrate: implications for chitin formation in molluscs. Int. J. Mol. Sci. 14, 11842–11860.
Shi, Y., Fan, Z., Li, G., Zhang, L., Yue, Z., Yan, X., Xu, A., Huang, S., 2020. The family of amphioxus chitin synthases offers insight into the evolution of chitin formation in chordates. Mol. Phylogenet. Evol. 143, 106691.
Suzuki, M., Nagasawa, H., 2013. Mollusk shell structures and their formation mechanism. Can. J. Zool. 91, 349–366.
Suzuki, M., Sakuda, S., Nagasawa, H., 2007. Identification of chitin in the prismatic layer of the shell and a chitin synthase gene from the Japanese pearl oyster, *Pinctada fucata*. Biosci. Biotech. Bioch. 71, 1735–1744.
Takeuchi, T., 2017. Molluscan genomics: implications for biology and aquaculture. Curr. Mol. Biol. Rep. 3, 297–305.
Tan, K., Zheng, H., 2020. Ocean acidification and adaptive bivalve farming. Sci. Total Environ. 701, 134794.
Tang, W.J., Fernandez, J.G., Sohn, J.J., Amemiya, C.T., 2015. Chitin is endogenously produced in vertebrates. Curr. Biol. 25, 897–900.
Thanos, C.D., Goodwill, K.E., Bowie, J.U., 1999. Oligomeric structure of the human EphB2 receptor SAM domain. Science 1979 (283), 833–836.
Vandepas, L.E., Tassia, M.G., Halanych, K.M., Amemiya, C.T., 2023. Unexpected distribution of chitin and chitin synthase across soft-bodied cnidarians. Biomolecules 13, 777.
Weiner, S., Talmon, Y., Traub, W., 1983. Electron diffraction of mollusc shell organic matrices and their relationship to the mineral phase. Int. J. Biol. Macromol. 5, 325–328.
Weiner, S., Traub, W., 1980. X-ray diffraction study of the insoluble organic matrix of mollusk shells. FEBS Lett. 111, 311–316.
Weiss, I., 2012. Species-specific shells: chitin synthases and cell mechanics in molluscs. Zeitschrift Für Kristallographie-Cryst. Mater. 227, 723–738.
Weiss, I.M., Schönitzer, V., Eichner, N., Sumper, M., 2006. The chitin synthase involved in marine bivalve mollusk shell formation contains a myosin domain. FEBS Lett. 580, 1846–1852.
Weiss, I.M., Lüke, F., Eichner, N., Guth, C., Clausen-Schaumann, H., 2013. On the function of chitin synthase extracellular domains in biomineralization. J. Struct. Biol. 183, 216–225.
Yabe, T., Yamada-Okabe, T., Nakajima, T., Sudoh, M., Arisawa, M., Yamada-Okabe, H., 1998. Mutational analysis of chitin synthase 2 of Saccharomyces cerevisiae: identification of additional amino acid residues involved in its catalytic activity. Eur. J. Biochem. 258, 941–947.
Zakrzewski, A.-C., Weigert, A., Helm, C., Adamski, M., Adamska, M., Bleidorn, C., Raible, F., Hausen, H., 2014. Early divergence, broad distribution, and high diversity of animal chitin synthases. Genome Biol. Evol. 6, 316–325.
Zhang, Y., Liu, Z., Song, X., Huang, S., Wang, L., Song, L., 2019. The inhibition of ocean acidification on the formation of oyster calcified shell by regulating the expression of *Cg*chs1 and *Cg*chit4. Front. Physiol. 10, 1034.
Zhao, X., Han, Y., Chen, B., Xia, B., Qu, K., Liu, G., 2020. CO_2-driven ocean acidification weakens mussel shell defense capacity and induces global molecular compensatory responses. Chemosphere 243, 125415.